Influence of a Lipid Interface on Protein Dynamics in a Fungal Lipase

Günther H. Peters* and Robert P. Bywater[†]

*Department of Chemistry, Membrane and Statistical Physics Group, (MEMPHYS), Technical University of Denmark,
DK-2800 Lyngby, Denmark; and [†]Biostructure Group, Novo Nordisk A/S, Novo Nordisk Park, DK-2760 Måløv, Denmark

ABSTRACT   Lipases catalyze lipolytic reactions and for optimal activity they require a lipid interface. To study the effect of a lipid aggregate on the behavior of the enzyme at the interfacial plane and how the aggregate influences an attached substrate or product molecule in time and space, we have performed molecular dynamics simulations. The simulations were performed over 1 to 2 ns using explicit SPC water. The interaction energies between protein and lipid are mainly due to van der Waals contributions reflecting the hydrophobic nature of the lipid molecules. Estimations of the protonation state of titratable residues indicated that the negative charge on the fatty acid is stabilized by interactions with the titratable residues Tyr-28, His-143, and His-257. In the presence of a lipid patch, the active site lid opens wider than observed in the corresponding simulations in an aqueous environment. In that lid conformation, the hydrophobic residues Ile-85, Ile-89, and Leu-92 are embedded in the lipid patch. The behavior of the substrate or product molecule is sensitive to the environment. Entering and leaving of substrate molecules could be observed in presence of the lipid patch, whereas the product forms strong hydrogen bonds with Ser-82, Ser-144, and Trp-88, suggesting that the formation of hydrogen bonds may be an important contribution to the mechanism by which product inhibition might take place.

INTRODUCTION

Biological membranes play multiple roles in cells by establishing the permeability barrier for cells and cell organelles by providing the matrix for the assembly and function of a wide variety of catalytic processes and by actively influencing the function of membrane-associated properties. Additionally, membranes serve as the matrix and support for a vast array of proteins involved in functions of the cells such as signal transduction, solute transport (via, e.g., ion channels), DNA replication, protein targeting and trafficking, or cell-cell recognition (Dowhan, 1997; Tocanne et al., 1994; Prenner et al., 1999; Lindeberg et al., 2000; Burden et al., 1999; Lindblom and Quist, 1998; Dumas et al., 1999; Mouritsen and Biltonen, 1993; Mouritsen and Jorgensen, 1998; Weers et al., 1999; Cantor, 1997). There are numerous examples in nature where the biological function of a wide range of proteins is associated with the binding mechanism toward a lipid interface, and these processes all require intimate interaction between lipid and proteins that have evolved to fulfill these special functions (Lindblom and Quist, 1998). As an example, the myristolated alanine-rich C-kinase substrate protein, which is an integral part of the signal transduction network, requires both the hydrophobic insertion of myristate into the lipid bilayer as well as the electrostatic interaction of basic amino acid residues with acidic lipids (Seykora et al., 1996). However, other important processes not involving membranes as such also work at the interfacial plane between lipid and water as in lipoprotein particles, in emulsions of dietary fats, and fat particles stored in adipose tissue.

An important class of enzymes, lipases, functions exclusively at the lipid-water interface. Two important members of the family are phospholipases and triglyceride lipases. Phospholipases generate second messengers, participate in cytotoxity, and hydrolyze phospholipids in the gastrointestinal tract. Triglyceride lipases (EC 3.1.1.3) are essential for transporting fats into cells for storage or for conversion into energy. Triglycerides in the diet, in lipoprotein particles, and in fat storage cells cannot be directly absorbed into cells. These esters must be hydrolyzed into free fatty acids and monoglycerols before they are able to cross the cellular membranes, and it is here where, for instance, lipases play an integral part of the absorption process and hence energy conversion.

The essential role of lipases in many biological processes has stimulated interest in elucidating the molecular details determining the function of triglyceride lipases (Wulfson, 1994). Not only the molecular basis of their catalytic function but also the mechanism by which these enzymes are activated are of interest (Peters, 2001a). Considerable insight has been obtained from crystal structures of the first two resolved lipase structures, human pancreatic lipase (Winkler et al., 1990), and *Rhizomucor miehei* lipase (Rml) (Brady et al., 1990), revealing that a surface loop (the lid domain) covers the active site, which is inaccessible to the solvent and substrate. Both lipases were later co-crystallized in the presence of either inhibitor (Brzozowski et al., 1991; Derewenda et al., 1992; Egloff et al., 1995) or mixed micelles (van Tilburgh et al., 1993) providing further insight in the phenomenon of interfacial activation. The crys-

tal structures indicate that the conformational changes during activation are rigid body hinge-type motions of single or multiple helices (Derewenda et al., 1994a,b). In the present study, we focus on Rml. Like other lipases, it has a catalytic center with a trypsin-like triad (Ser· · ·His· · ·acidic residue). The active site is shielded from the solvent by a helical loop, which in the literature is referred to as a "lid." During activation, the lid is displaced to allow access of the substrate to the active site. From the crystal structures, it is evident that not only does the backbone of the central part of the lid moves by more than 7 Å but also that the hydrophobic surface increases by ~750 Å^2 (Derewenda et al., 1992), which agrees well with the general observation that, in an aqueous solution, the lipase activity is increased as the substrate concentration is higher than the micelle concentration (Panaiotov et al., 1997; Peters et al., 1997a).

This phenomenon of interfacial activation could be regarded as an evolutionary response to the requirement to hydrolyze insoluble substrates. This property distinguishes lipolytic proteins from esterases, which catalyzes the digestion of soluble esters. The mechanism of interfacial activation is a unique property of lipases. Already in the early sixties it has been postulated that conformational changes occur in lipases upon activation (Desnulle et al., 1960; Sarda and Desnuelle, 1958). Many mechanisms have been proposed to explain the activation of lipases at a lipid-water interface ranging from a surface-mediated process in which preexisting interfacial properties of the substrate governs the behavior of lipolytic enzymes to a mechanism based on the conformational changes in the enzyme upon adsorption on to the interface (Derewenda et al., 1994b; Thuren, 1988; Muderhwa and Brockman, 1992). With the increasing amount of information, it becomes clear that these models are merely conceptual extremes and not mutually exclusive (Peters et al., 2000). Consequently, it is important also to understand the physics and the chemistry that relate the structural fold of the protein and the structure of the binding site with the function and action of the enzyme. Substrate binding, enzymatic processes, and product release are often associated with conformational changes in the structure, and these structural changes require a certain flexibility of the protein (Zidek et al., 1999; Peters et al., 2001b; G.H. Peters and R.P. Bywater, submitted). Therefore, an essential aspect of protein function is the dynamic response of the protein upon substrate binding and product release. Our previous studies focused either on studying the phases and interfacial properties of the lipid substrate (Peters et al., 1995a,b) or on lipases (Peters et al., 1996a,b, 1997b). To gain further insight in the structure-function relation of the Rml, we have performed molecular dynamics simulations of Rml in complex with a substrate or a product molecule in the presence of a lipid aggregate. Interaction energies, protonation state of titratable residues, and protein flexibility were monitored along the trajectories providing insight how substrate, product, and enzyme complexed with substrate or product molecule behave in time and space when located at a lipid interface.

MATERIALS AND METHODS

Starting structures

The crystal structure of the Rml complexed with an inhibitor and solved to 2.6-Å resolution (Brzozowski et al., 1991) was used as a model for the active structure. The structure was obtained from the Protein Data Bank (Bernstein et al., 1977), entry code 4tgl. In this structure, the inhibitor 2 diethylphosophate is covalently bound to the active site serine, revealing the hydrophobic groove where the alkyl chain of the substrate is placed during catalytic reaction (Derewenda, 1994) and hence the possible binding mode of a substrate. We have used the inhibitor structure as a template to place either a product molecule (octanoate) or a substrate molecule (ethyl-octanoate) in the binding groove. The alkyl chain was placed in an all-trans conformation using the QUANTA software package (CHARMm, 1992). In our previous investigation, where we have investigated among other things the effect of charged or neutral fatty acid on the binding behavior and protein dynamics, we concluded that a negatively charged fatty acid molecule is favored in the binding cleft (Peters et al., 2001). To study the behavior of the protein in the presence of a lipid patch, we have placed 29 ethyl-octanoate molecules above the binding pocket.

Molecular dynamics simulations

The simulations (carried out using the parallelized C (charged) version of the GROMOS forcefield (Europort-D, 1997; van Gunsteren and Berendsen, 1987) on an 18-processor SGI Challenge) were performed using periodic boundary conditions with a truncated octahedron central cell and explicit SPC water (4930 molecules; Berendsen et al., 1987). The simulations lasted for at least 1 ns and were conducted at a temperature of 300 K. Nine (simulation with substrate) or 10 (simulation with product) water molecules at the lowest electrostatic potential were replaced by sodium ions to neutralize the system. Details of the molecular dynamics protocol have been presented elsewhere (Peters et al., 1996b). Examinations of the molecular structures and analyses of the trajectories were performed using the WHAT IF modeling program (Vriend, 1990) and the essential dynamics routines supplied therein. Analyses of the different geometrical properties (radius of gyration, number of hydrogen bonds, root mean square displacement (RMSD), surface accessibility, number of residues in random coil conformation, number of strained dihedrals) indicated that these properties remain constant after ~300 ps, and consequently, the final 600 ps of the trajectories were used for analyses.

Essential dynamics

Protein motions and flexibility were analyzed using the essential dynamics method. This technique has been described several times in the literature, and the reader is referred to one of the references (Amadei et al., 1993; Balsera et al., 1996; van Aalten et al., 1995; Peters et al., 1996b). Briefly, the method is based on the diagonalization of the covariance matrix constructed from the atomic displacements (Amadei et al., 1993; Ichiye and Karplus, 1991), resulting in a set of eigenvectors (describing a direction in the high-dimensional configurational space) and eigenvalues (represent the mean square fluctuation of the total displacement along the eigenvectors). Motions along the first few eigenvectors are mainly large anharmonic fluctuations and generally can be linked to the biological function of proteins (Amadei et al., 1993; van Aalten et al., 1996). Eigenvalues at higher indices represent harmonic (Gaussian) fluctuations, which are thermal fluctuations in nature. The different trajectories were compared using the so-called combined analysis (van Aalten et al., 1995), where the

trajectories, fitted on the same reference structure are concatenated, and a covariance matrix is constructed from the combined trajectory. Here, this technique is applied to the concatenated trajectories of the simulations of Rml complexed with substrate or product molecule in the presence of a lipid patch or an aqueous environment.

Electrostatic calculations

Electrostatic properties were determined by calculating pK_As of the titratable amino acids in the enzyme-binding pocket and of the product. These pK_As were estimated using the so-called single-site titration model (Antosiewicz et al. 1994) as described elsewhere (Antosiewicz et al., 1994; Peters et al., 1998). The methodology is based on the evaluation of the potential field at each titratable group, which is calculated by numerically solving the finite difference linearized Poisson-Boltzmann equation using an incomplete Cholesky preconditioned conjugate gradient method as implemented in the UHBD program (Madura et al., 1995; Davis et al., 1991). These potentials are then used to estimate the relative free energies and subsequently the apparent pK_As. The pK_As were estimated using the *Hybrid* procedure (Gilson, 1993). This method determines values for the pK_As, the charges of the protein and single sites, and the electrostatic energies as a function of pH. *Hybrid* is based on the separation of ionizable groups into clusters, where the interaction between ionizing charges within a cluster is treated exactly and intercluster interactions are approximated (Gilson, 1993). The atoms of the protein were assigned point charges and radii from the modified CHARMm22 force field (Antosiewicz et al., 1994). The dielectric constant of the solvent was set to $\epsilon = 80$, and that of the molecular interior was $\epsilon = 20$ as suggested by Antosiewicz et al. (1994). The relative dielectric constant was "smoothed" at the molecular surface so that it changed gradually between the protein and solvent values (Davis and McCammon, 1991). An ionic strength of 0.15 M, corresponding roughly to physiological conditions, was used in the calculations for the aqueous solution. A detailed description of the parameters used in these calculations have been published elsewhere (Peters et al., 1998, 1999).

RESULTS AND DISCUSSION

The activation of Rml, which involves the displacement of a helical loop, occurs at a hydrophobic interface such as lipid assemblies, micelles, monolayers, or bilayers. This structural rearrangement concomitantly creates a hydrophobic lipid-binding surface and allows the substrate to approach the active site. In an aqueous solution, the lid displacement is presumably thermodynamically unfavorable because of a relatively large hydrophobic patch that would necessarily be exposed as a result. Conversely, in the presence of hydrophobic interfaces, such as lipid aggregates, this nonpolar surface would be favored, and hence the open conformation of the lid would be stabilized. The overall catalytic process involves adsorption of the enzyme from the bulk aqueous phase to the lipid surface, activation of the enzyme, and catalysis in the water-lipid interface (Peters et al., 2000). Presumably, the binding of the substrate molecule and the release of the product may occur at the water-lipid interface. Such a process is difficult to probe by experiment, and we therefore have resorted to molecular dynamics to explore the behavior of the enzyme at the water-lipid interface. In particular, we are interested in the changes in the flexibility of the enzyme due to the presence of a lipid interface.
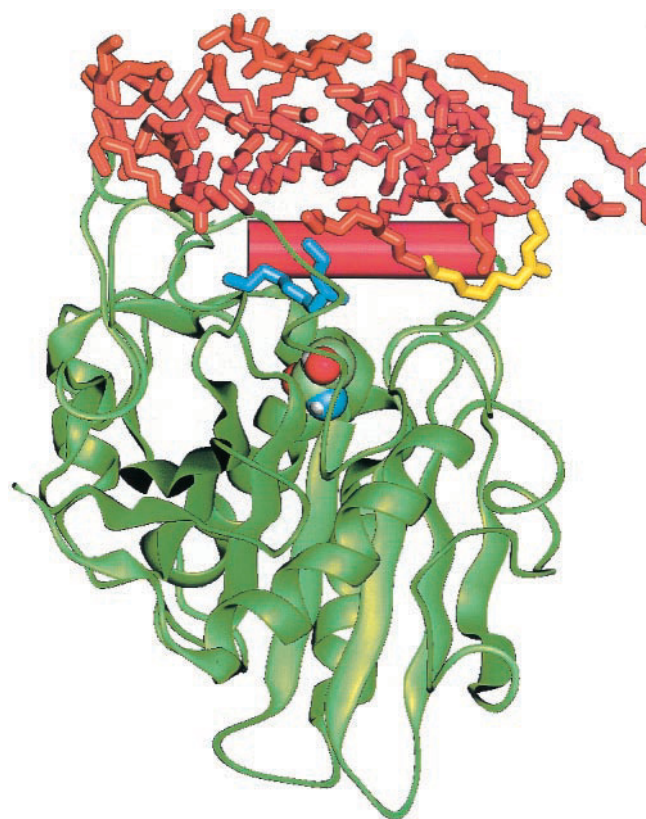

FIGURE 1 Secondary structure of Rml complexed with a substrate molecule and in the presence of the lipid patch consisting of substrate molecules. Active site lid is shown in red as a rod, whereas atoms of the active serine are displayed in the van der Waals modus. Color coding is as follows: green, red, blue, and white represent carbon, oxygen, nitrogen, and hydrogen atoms, respectively. The substrate molecules are displayed in sticks and are colored red, blue, or yellow. See text for more details.

Earlier results of an essential dynamics analysis on a wild-type lipase in polar or nonpolar solvent have been described elsewhere (Peters et al., 1996b). These studies were later extended to investigate the effect of ligand-induced perturbations on the protein dynamics (Peters et al., 1997b) and residues located in the binding pocket (Peters et al., 2001b). We showed that there is pronounced motion in the lid and that, as also found for other proteins, there are only a few essential eigenvectors describing protein motions of anharmonic nature, which are generally thought to govern the biophysical function of proteins. These earlier simulations were performed in either aqueous or nonpolar solvents. Here, we have extended our studies to focus on the structural and energetic properties of the protein in the presence of a lipid patch, which represents the true biochemical conditions under which these enzymes operate and with a substrate or product molecule bound at the active site. The substrate was ethyl-octanoate, identical to the molecules making up the lipid patch.

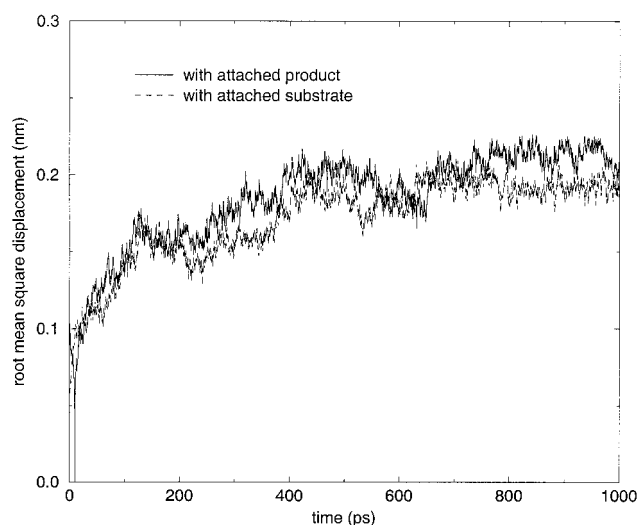The starting configuration of Rml-substrate structure used in the simulation is shown in Fig. 1, where Rml is

FIGURE 2 RMSDs of Cα coordinates as a function of simulation time for the Rml-product and Rml-substrate simulations in the presence of a lipid patch.
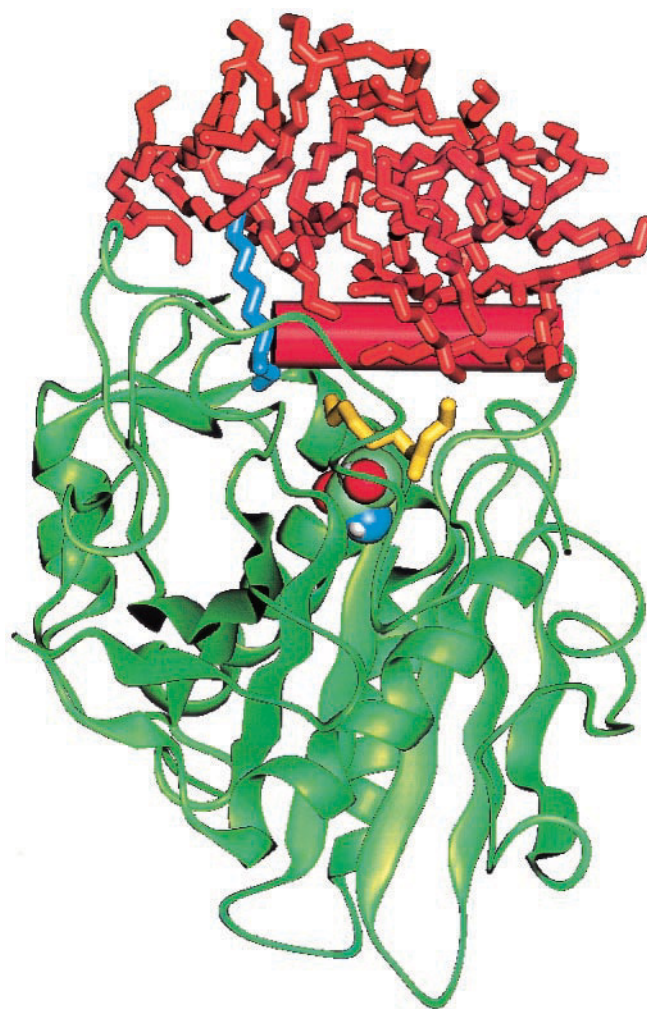

FIGURE 3 Snapshot of Rml and lipid molecules taken after 1000 ps. Color coding and display mode are the same as in Fig. 1. The blue-colored lipid molecule left the binding cleft, whereas the yellow colored substrate molecule has entered the cleft and approaches the active serine.

displayed in the open conformation. The binding cleft is covered by substrate molecules, and one substrate molecule (colored blue) is located in the binding pocket. The surrounding substrate molecules are placed randomly resembling a lipid aggregate (i.e., lipid patch). The same setup of the lipid patch was used for the Rml-product simulation. However, as discussed below, this simulation was extended and performed for 2 ns. The stability of the simulations was checked by computing inter alia the RMSD calculated with respect to the starting structure. RMSD shown in Fig. 2 indicate that both simulations are comparable in terms of having similar RMSD and that stable trajectories are reached after ~300 ps.

Visualization of several snapshots along the trajectories reveals some very intriguing features reflecting the dynamic behavior of the lipid molecules. During the course of the Rml-substrate simulation, a substrate molecule enters the binding cleft, whereas another substrate molecule leaves the pocket. The final snapshot taken after 1000 ps is shown in Fig. 3, which should be compared with the initial configuration in Fig. 1. The entering and leaving molecules are colored yellow and blue, respectively. Significantly different is the behavior of the product molecule. As discussed in detail below, the product molecule forms hydrogen bonds to residues located in the vicinity of the active site, and even over the simulation period of 2 ns the molecule is not leaving the binding pocket. Over this period several substrate molecules enter the pocket but are not able to push out the product molecule. Interestingly, most of the substrate molecules enter the groove at the active site loop region around Pro-96–Val-107, which we have identified earlier as a potential gateway in the activation of Rml (Peters et al., 1996b). To our knowledge, this is the first time that such

material transfer has been observed in a molecular dynamics simulation. However, we concede that a simulation of much longer duration is required to establish this observation in statistically significant way.

One of the most fundamental questions is how the protein flexibility is affected by the presence of a lipid interface. To study this effect, we have used the essential dynamics technique (Amadei et al., 1993). Changes in the protein dynamics due to the presence of product or substrate molecules were studied by performing a combined analysis of the concatenated trajectories (van Aalten et al., 1995). Differences in the essential subspace can be studied by projecting the separate trajectories onto the combined eigenvectors. The average of the projections and the mean square fluctuations in these projections as a function of eigenvector indices are shown in Fig. 4. The average projection (Fig. 4 *A*) shows differences in equilibrium structure, whereas the

A

B

C
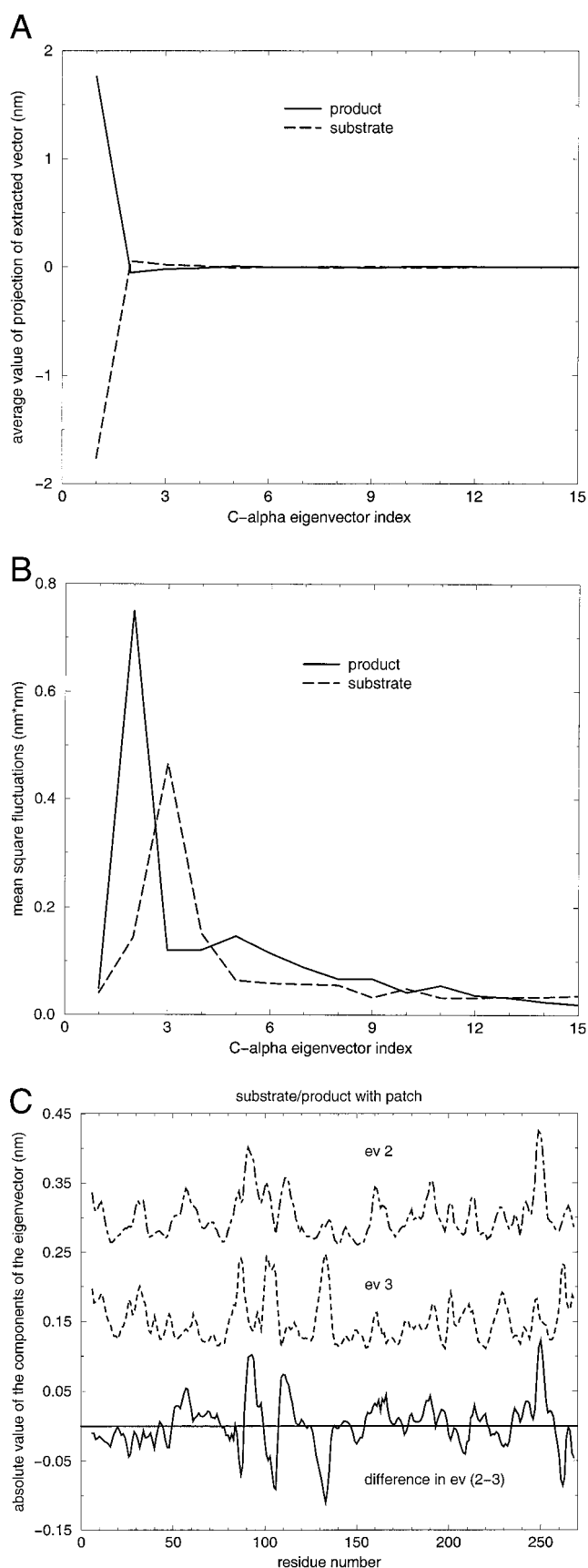
mean square fluctuation (Fig. 4 *B*) can be used to study differences in protein flexibility. The structural changes are predominately caused by partially closing of the active site lid observed in the Rml-product simulation. These conformational changes involve the regions His-207–Phe-215, Ile-89–Val-93, and Trp-38–Leu-49. The flexibility of the latter region (although not close to the active site lid) has been proposed to correlate to the active site lid motion (Peters et al., 1996b). Significant differences in protein motions are observed along eigenvectors 2 and 3 (Fig. 4 *B*). Motions in the subspace spanned by eigenvector 2 are predominately observed in the Rml-product simulation, whereas motions along eigenvector 3 are predominately found in the Rml-substrate simulation. Absolute values of the eigenvectors 2 and 3 as well as the difference between these two eigenvectors as a function of residue numbers are shown in Fig. 4 *C*. The observed difference in the protein dynamics reflects the behavior of the substrate and product molecules. In the Rml-substrate simulation, substrate molecules enter and then leave the binding groove, whereas in the Rml-product simulation, formation of hydrogen bonds between the carboxylate group of the product molecule and residues located in the binding cleft can be clearly observed. Hence, differences in protein dynamics are mainly monitored in the region of the active site lid. Choosing arbitrarily a threshold of >0.03 nm for the absolute value, we can identify protein segments that are predominately flexible in the Rml-product or in the Rml-substrate simulations. In the Rml-product simulation, these regions are Ser-56–Ile-59, Ala-90–Val-95, His-108–Ser-114, Tyr-187–Thr-191, and Ile-248–Thr-252, whereas in the Rml-substrate simulation, the regions are Arg-86–Trp-88, Pro-101–Val-107, Asp-128–Ser-135, His-207–Pro-210, and Tyr-260–Asn-264.

The previous analyses are based on simulations in which a lipid patch is present. To further elucidate the influence of the lipid patch on the flexibility of the protein, we compare below the present results with the trajectories obtained from Rml-substrate and Rml-product simulations in an aqueous environment. Analyses are performed for Rml-substrate simulations with and without a lipid patch (Figs. 5 *A* and 6 *b*) and Rml-product simulations with and without a lipid patch (Figs. 5 *B* and 6 *c*). Essential dynamics analyses of the corresponding concatenated trajectories reveal structural changes in the subspace spanned by eigenvector 1 and difference in protein dynamics along eigenvectors 2 and 3.

FIGURE 4 Average values (*A*) and mean square fluctuations (*B*) of the projections of the Rml-product and Rml-substrate trajectories onto the eigenvectors extracted from the Cα coordinates covariance matrix of the concatenated trajectories as a function of the eigenvector index. (*C*) Absolute value of the eigenvectors 2 and 3 obtained from the Cα coordinates covariance matrix as a function of the coordinate number (individual curves are shifted in *y* direction). The bottom curve displays the differences between eigenvectors 2 and 3.
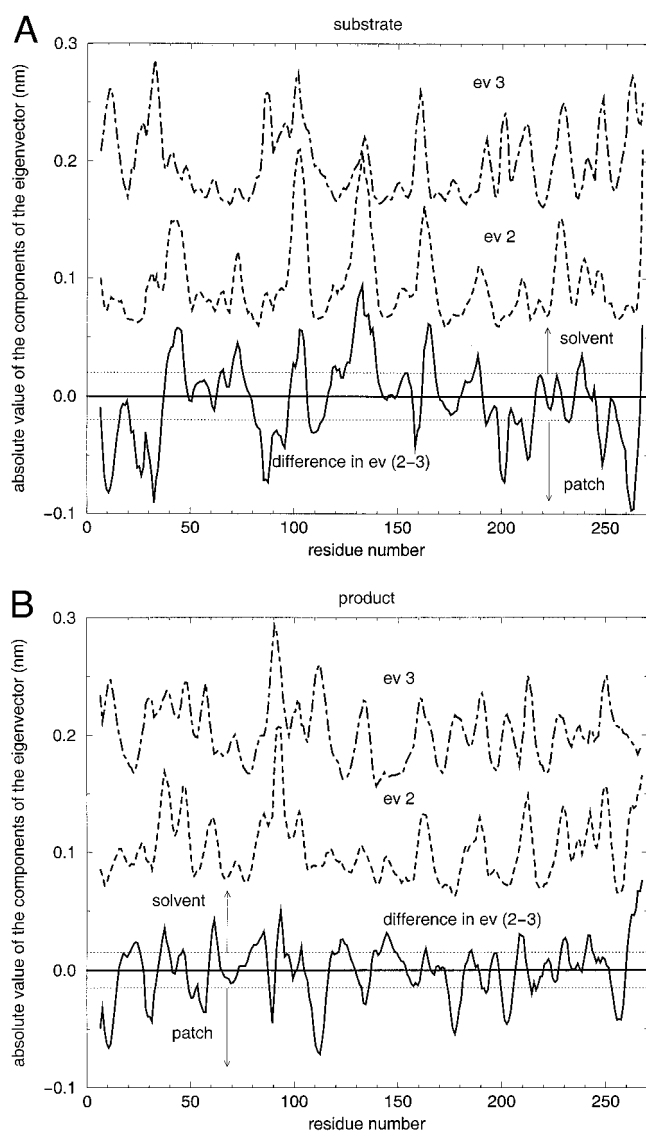
FIGURE 5 Effect of the protein environment on the protein flexibility in the Rml-substrate (*A*) and Rml-product (*B*) complexes. Protein motions were extracted from the Rml-substrate or Rml-product complex in the presence of a lipid patch or an aqueous environment. The graphs display the absolute values of the eigenvectors 2 and 3 obtained from the Cα coordinates covariance matrix of the concatenated trajectories as a function of the residue number. The lower curves in both figures show the differences between the two respective eigenvectors. These curves reflect the difference in protein dynamics in the Rml-substrate (*A*) or Rml-product (*B*) complex due to the presence of a lipid patch or an aqueous environment.

Conformational changes involve the regions Val-32–Gly-35, Thr-37–Ala-45, Thr-57–Thr-62, active site lid and hinge regions, Pro-209–Gly-214, Thr-236–Glu-240, and the N-terminal part. These regions are displayed in Fig. 6 *a*. The conformational changes observed in the Rml-substrate and Rml-product simulations are similar and mainly deviate in the magnitude (data not shown). The presence of the lipid patch causes the active site lid to open wider than observed in an aqueous environment.

To further quantify the lid opening, we have calculated the root square displacement between the lid conformation in the crystal structure (PDB id.: 4tgl) and configurations taken from the trajectory of the Rml-product-patch simulation. RMSD values are shown in Fig. 7 and selected snapshots of lid conformations are displayed in Fig. 8. The solid curve in Fig. 7 is the RMSD for the active site lid region Ile-77–Tyr-99, whereas the dashed line refers to the segments Ile-77–Ile-89 and Val-95–Tyr-99. Significant contribution to the RMSD data stems from the loop region Ala-90–Phe-99, which rearranges resulting in loop conformation where the hydrophobic side chain of the residues Ile-85, Ile-89, and Leu-92 reach into the lipid patch. Similar observations were made in simulations using Brownian dynamics (Peters et al., 1996a). This rearrangement is also observed in the snapshots displayed in Fig. 8. These images are taken at 450, 1130, and 2000 ps and according to Fig. 7 represent configurations with low, high, and medium RMSD values, respectively.

Absolute values of the eigenvectors 2 and 3 as well as the difference between these two eigenvectors as a function of residue number are shown in Fig. 5, *A* (Rml-substrate) and *B* (Rml-product). The regions, which show relatively high flexibility, are displayed in Fig. 6 *b* (Rml-substrate) and *c* (Rml-product) and colored as follows: yellow refers to motions predominately observed in an aqueous environment and dark blue refers to motions predominately observed in the presence of a lipid patch. The subtle differences reflect the different behavior of substrate or product molecules due to the environment. Entering and leaving of substrate molecules were only observed in the Rml-substrate-patch simulation. However, in a purely aqueous environment, the substrate molecule remained in the binding cleft (Peters et al., 2001a) taking a configuration similar to the one we have observed earlier in our studies with methyl hexanoate (Peters et al., 1996b). Independent of the environment, the product molecule does not leave the pocket. In the Rml-product-patch simulation the tail of the fatty acid points outward into the hydrophobic patch and the carboxylate group forms hydrogen bonds with residues in the binding cleft. Contrarily, in an aqueous environment the product remains in the binding cleft with the hydrophobic tail aligning to Leu-208–Pro-210 (Peters et al., 2001). In Fig. 9 (Rml-substrate-patch) and 10 (Rml-product-patch), we have monitored the distance between the active site (Ser-144) and substrate molecules, which along the trajectory have been at one time within a distance of at least 1 nm to Ser-144. The picture, which emerges from these distances, is quite dynamic, where substrate molecules constantly enter the binding cleft. Clearly, the fatty acid molecule remains in the binding pocket over the 2-ns simulation (Fig. 10 *a*) and entering substrate molecules (Fig. 6, *b–d*) are not able to force out the product molecule. In contrast, in the Rml-substrate-patch simulation, a substrate molecule entering
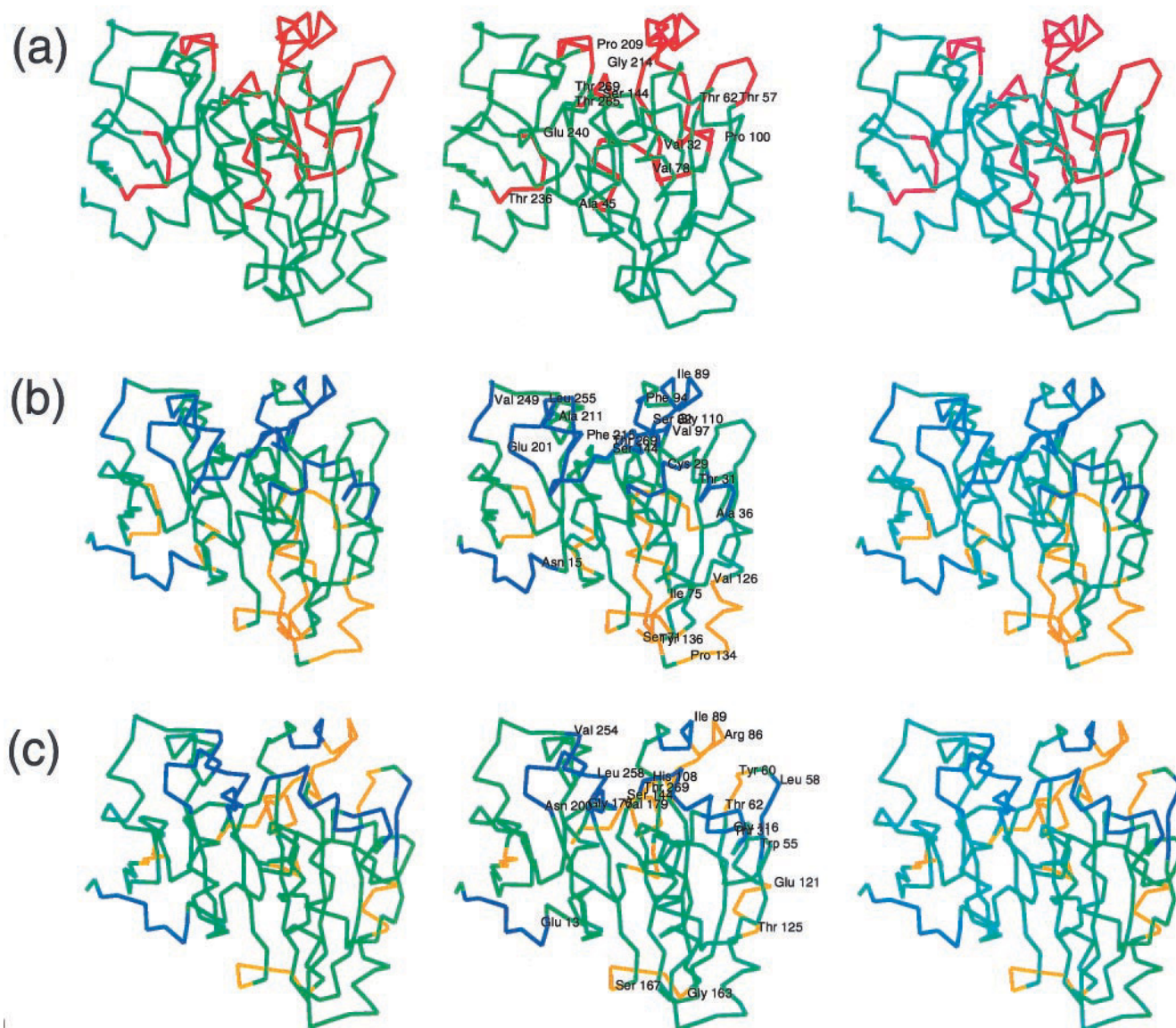
FIGURE 6   Three-dimensional stereo-plots displaying the protein regions where conformational changes or different protein flexibility occur due to the presence of the product or substrate in the simulations with the lipid patch. (*a*) Regions, where conformational changes occur, are colored red. These region correspond to the results of Fig. 4 *A*. *b* (Rml-substrate) and *c* (Rml-product) show the effect of the protein environment on the protein flexibility and correspond to the results of Fig. 5 *A* and *B*. The structural parts colored yellow and blue display flexible segments, which are predominately observed along eigenvectors 2 (aqueous environment) and 3 (lipid patch), respectively.

from the lipid patch is able to push out a substrate molecule from the binding pocket (see Figs. 1, 3, and 9).

The protein dynamics extracted from the essential dynamics analyses are correlated motions (Amadei et al., 1993). As shown by our analyses of the protein flexibility in the presence of substrate or product molecules surrounded by water or lipid (Figs. 5 *B* and 6 *b*), the distances between residues involved in the correlated motions are beyond simple van der Waals contacts. Clearly, this implies that the correlated motions are transmitted by either the specific protein fold (i.e., mechanistic origin) or by a tight water

network formed around the active site. The presence of the lipid patch reduces the number of water molecules in the vicinity of the protein surface and interaction energies between protein or ligand, and bound water molecules are significantly smaller than the corresponding protein-lipid interactions. As discussed above, in the simulations with the product or substrate molecules present in the binding cleft and surrounded by substrate molecules (i.e., patch), we could observe the entering and leaving of lipid molecules. Consequently, interaction energies between the protein and single lipid molecules vary significantly during the simula-
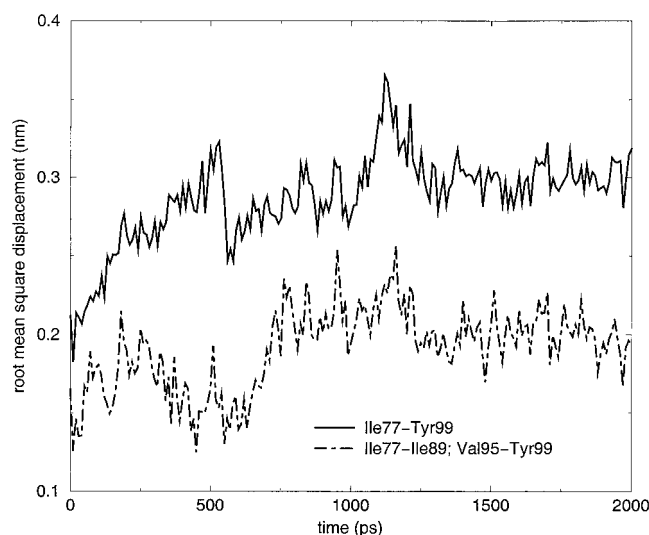
FIGURE 7 RMSDs between the active site lid (Ile-77–Pro-101) in the crystal structure (4tgl) and lid conformations taken along the trajectory from the Rml-product-patch simulation as a function of simulation time.

tions. We therefore decided to calculate the electrostatic and van der Waals interactions between the protein and all lipid molecules. The individual energy contributions to the protein-lipid interactions as functions of simulation time are shown in Fig. 11. As expected, due to the hydrophobic nature of the lipid molecules, the van der Waals interaction energies are significantly lower than the electrostatic energies and are comparable for the product and substrate molecules. The relatively large contribution to the electrostatic protein-product-lipid interactions stems from the negatively charged carboxylate group of the fatty acid molecule. The electrostatic protein-product-lipid energy decreases significantly within the first 200 ps. To understand the origin of the decrease in the electrostatic energy, we have monitored several distances between the product molecule and key residues in the binding pocket located in the vicinity of the fatty acid molecule. Distances between the carboxylate group of the fatty acid and Ser-144, Ser-82, Trp-88 as a function of simulation time are shown in Fig. 12. Furthermore, to follow the motion of the hexyl chain of the product molecule during the simulation, the distances between the tail (CA-6) and the residues Phe-111 and Leu-145 were monitored (Fig. 12). As seen from the increased Phe-111–CA-6 and Leu-145–CA-6 distances, the tail of the product molecule moves outward from the binding cleft into the lipid patch. The carboxylate group, on the other hand, forms hydrogen bonds with Ser-82, Ser-144, and Trp-88. Initially, the simulation was performed for 1 ns, and we hypothesized that the hydrogen pattern may break after a longer simulation period. We therefore extended the simulation to 2 ns. However, as indicated in Fig. 12, the hydrogen bonds between the carboxylate group and the serine residues persist over the 2-ns simulation period (see upper two graphs in

Fig. 12). For these residues the only changes could be observed in the hydrogen bond patterns; i.e., the residues bound to either of the oxygen atoms in the carboxylate group of the fatty acid molecule. Tight hydrogen bond patterns are observed between the serine residues and the carboxylate group of the fatty acid, whereas the tendency to form hydrogen bonds with the tryptophan residue is less stable due to its flexibility. In Fig. 13, the time evolution of the hydrogen bond pattern are indicated by the selected configurations taken from the trajectory. As mentioned above the product molecule (fatty acid) forms strong hydrogen bonds with Ser-82 and Ser-144, and therefore the carboxylate group is relative fixed in space. Contrary, the carbon chain is relatively flexible, exploring several locations in the binding pocket and conformation in the lipid patch. The strong tendency of the carboxylate moiety of the fatty acid molecule to form hydrogen bonds with residues in the binding pocket could be a mechanism by which product inhibition takes place. This may further explain the experimentally observed inhibitory effect of fatty acid on the catalytic reaction of the bacterial lipase *Pseudomonas cepaeia,* the yeast lipase *Candida rugosa,* and the fungal lipases *R. miehei* and *Rhizopus delemar* (Peters et al., 2000). In this study, fluorescence microscopy, surface potential, and activity measurements were used to investigate the influence of fatty acid among other lipids on the activity of these lipases. The results indicated that the level of inhibition of the fatty acid correlates with the lateral lipid distribution, interfacial properties of the lipid interface and the isoelectric point of the enzymes (Peters et al., 2000). The simulations performed here point to an additional important factor that of product inhibition.

Visualization and distance analysis have led to the identification of potential hydrogen bond partners. Another contribution to the binding of the negatively charged fatty acid is the interaction with ionizable side chains. The structural inhomogeneity may not only influence ligand binding by entropic contributions, but may also change the electrostatic environment of a titratable residues causing the protonation state (pK_A) of that side chain to vary over a wide range. This variation could be important because pK_A shifts have been linked to enzymatic catalysis, substrate binding, and protein-protein association (Warshel and Russell, 1984; Warshel and Åqvist, 1991; Antosiewicz et al., 1994; Honig and Nicholls, 1995).

We have applied the single site titration method (Antosiewicz et al., 1994) and have calculated the pK_As of titratable residues along the trajectory. The electrostatic calculations and estimations of the pK_As were performed using the UHBD program (Madura et al., 1995; Davis et al., 1991) and the *Hybrid* procedure developed by Gilson (1993). This method yields both accurate energies and fractional charges of titratable sites (Gilson, 1993). Our calculations, in particular, focused on the protonation state of titratable amino acids located in the binding pocket as well
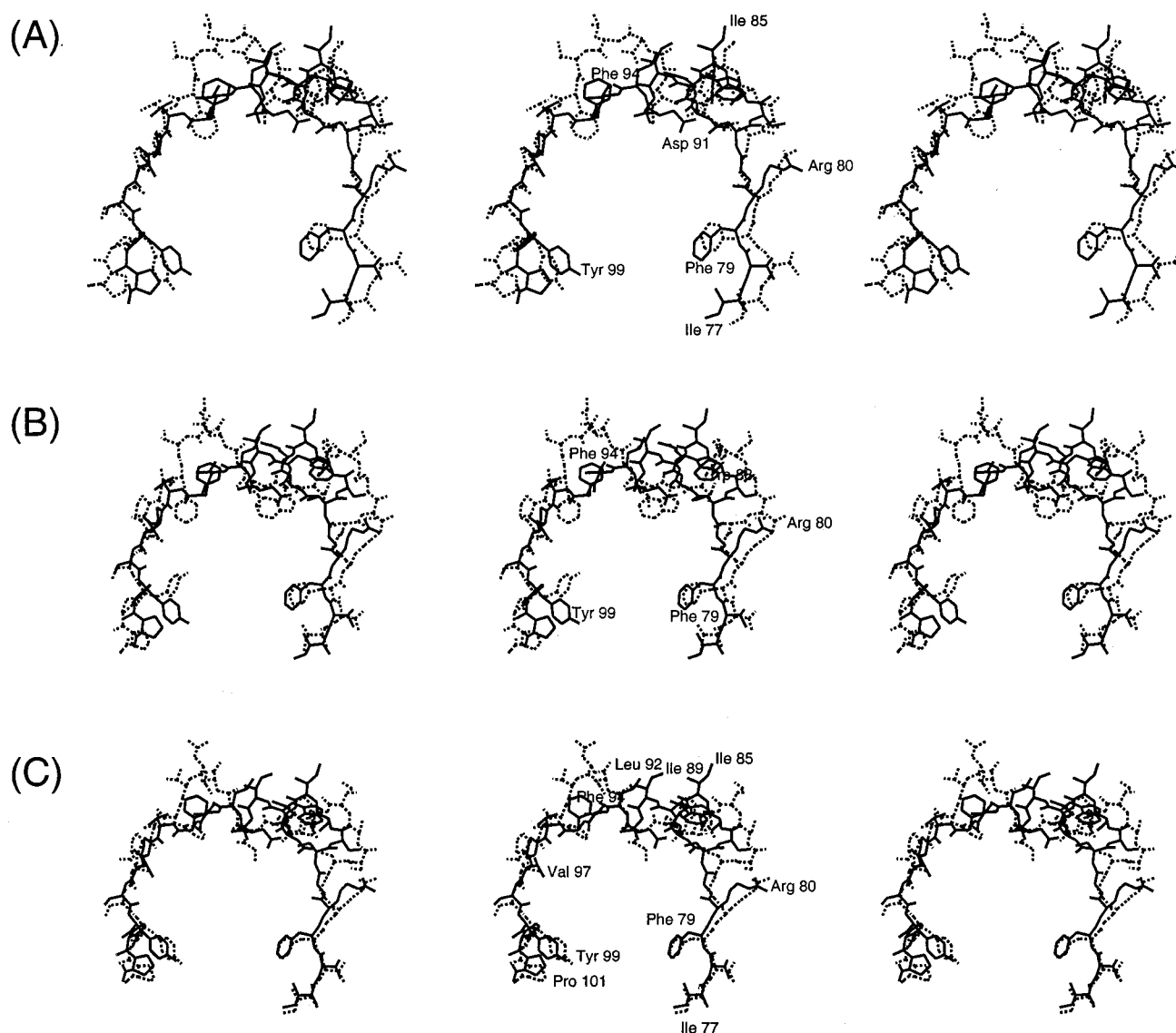
FIGURE 8   Three-dimensional stereo-plots showing the difference between the active site lid (Ile-77–Pro-101) taken from the crystal structure (4tgl) and lid conformations taken along the trajectory from the Rml-product-patch simulations. Solid curve represents the active site lid from the crystal structure, whereas the dash line represents lid configurations at 450 (*A*), 1130 (*B*), and 2000 ps (*C*).

as the carboxyl group of the product. Hence, the calculations were performed with the product molecule present in the binding pocket to 1) estimate the influence of flexibility on the protonation state of the fatty acid and to 2) determine the interaction energies between the carboxyl group of the fatty acid molecule and titratable residues in the binding pocket. There are six titratable residues: Tyr-28, His-143, Arg-197, Asp-203, His-257, and Tyr-260, which interact significantly with the carboxylate group. The time evolution of these interaction energies is shown in Fig. 14. Three residues (Tyr-28, His-143, and His-257) have a strong interaction, defined here as >5 kJ/mol with the fatty acid moiety. The dipole of the O-H (Tyr-28) and the N-H (His-

143 and His-257) stabilizes the negative charge on the carboxylate group of the fatty acid molecule. There are relatively larger fluctuations in the interaction energies between the carboxylate group (COO^-) of the product and Tyr-28 than observed for the interaction energies His-143-COO^- or His-257-COO^- reflecting the flexibility of the tyrosine side chains. The reasoning for the relative stiffness of the His residues is twofold. First, His-143 and His-257 are buried deeper in the binding pocket than the Tyr-28, and second His has an additional hydrogen bond functionality that is typically occupied in hydrogen bonding to other groups in the protein or to water. Although these interaction energies contribute to attracting the carboxylate group to the
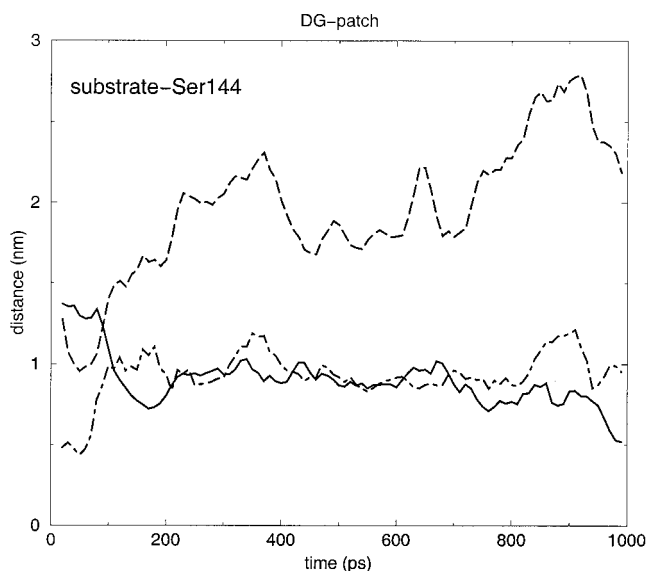
FIGURE 9 Rml-substrate-patch simulation. Distance between the active site Ser-144 (hydroxyl group) and substrate molecules (oxygen ester bond), which along the trajectory have been at one time within a distance of at least 10 Å to Ser-144. The three lines correspond to three different substrate molecules.

binding groove, it appears from Fig. 12 that hydrogen bonding between the carboxylate group of the fatty acid molecule and Ser-82/Ser-144 are the major contributions (as
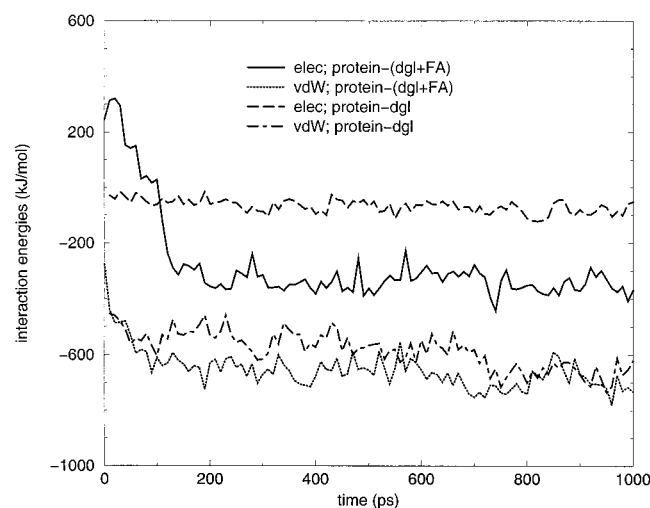

FIGURE 11 van der Waals and electrostatic interaction energies between Rml and substrate or Rml and product are shown as a function of simulation time.

seen from the constant hydrogen bond distances in Fig. 12) to prevent the release of the product.

CONCLUSION

Microbial lipases have attracted considerable attention owing their capability of catalyzing a wide variety of reactions.
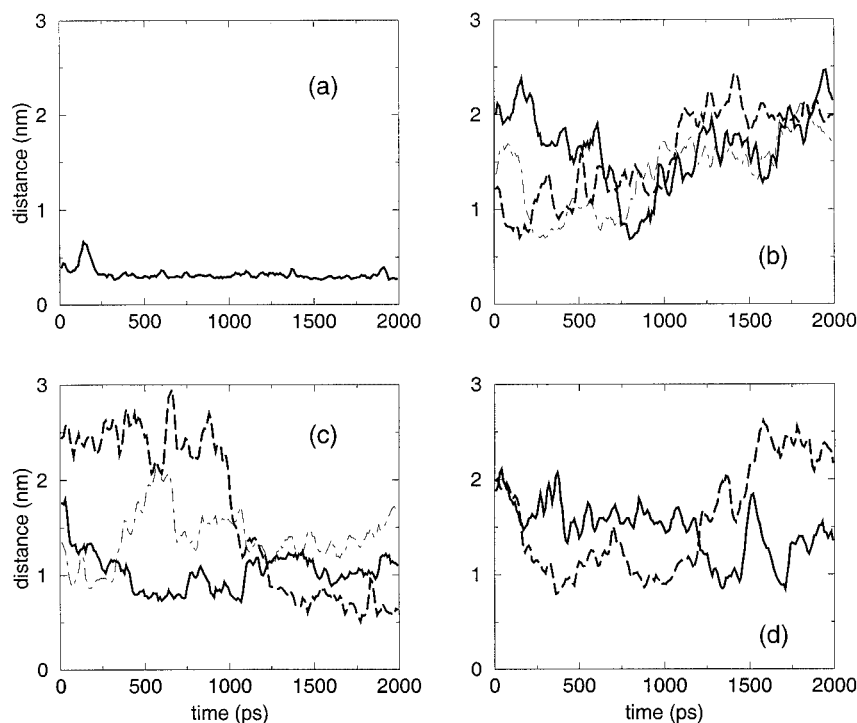

FIGURE 10 Rml-product-patch simulation. (*a*) Distance between carboxyl group of the product and Ser-144. (*b–d*) Distances between Ser-144 and different substrate molecules (see Fig. 9 legend for more details). For clarity only a maximum of three molecules have been displayed in each figure.
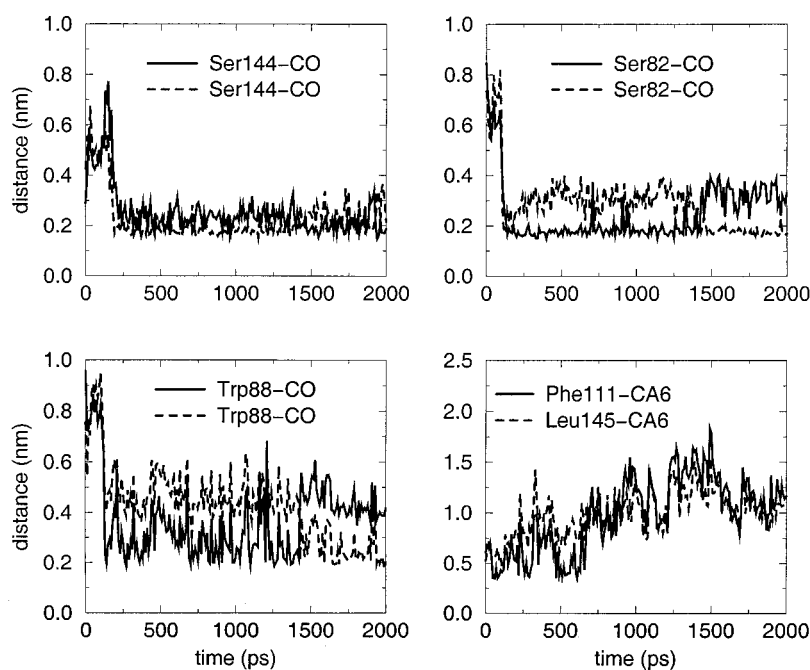
FIGURE 12 Selected distances between atoms in the binding cleft of Rml and the oxygen atoms of the carboxylate group of the product molecule (fatty acid). The protein atoms are HG (Ser-144), HG (Ser-88), HE1 (Trp-88), CD1 (Phe-111), and CD2 (Leu-145).

These enzymes obtain optimal activity only in the presence of a lipid interface. To access the importance of flexibility

under these conditions, we have performed molecular dynamics simulations of Rml complexed with a substrate
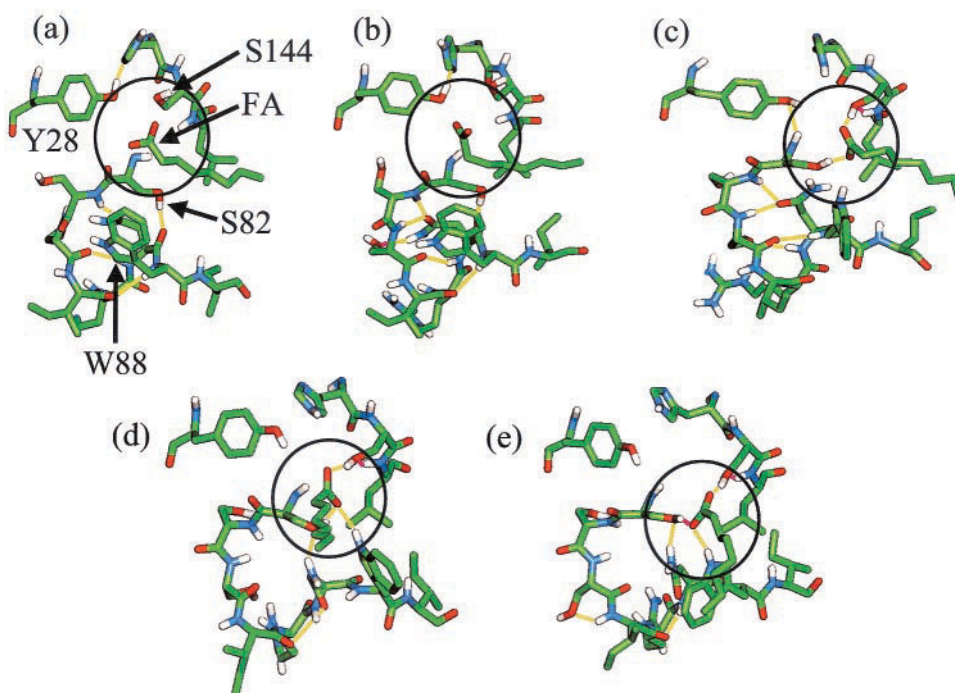

FIGURE 13 Snapshots taken along the trajectory from the Rml-product-patch simulation showing the hydrogen bond pattern between the carboxylate group of the product molecule and residues in the binding pocket. Hydrogen bonds are shown as red solid bonds. The snapshots are taken at 0 (a), 50 (b), 600 (c), 1230 (d), and 1940 ps (e).
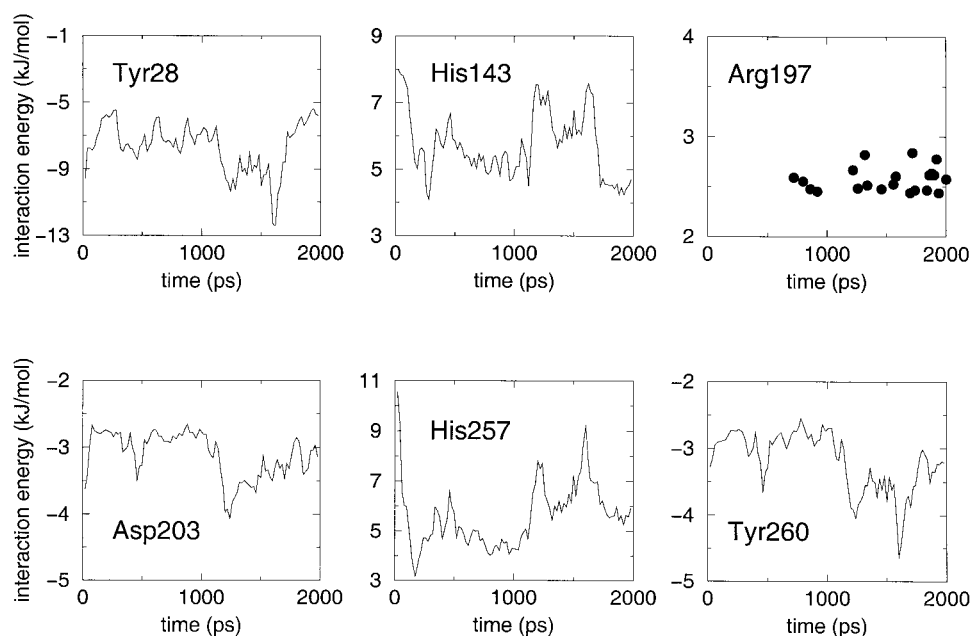
FIGURE 14 Electrostatic interaction energies between the ionizable groups (Tyr-28, His-143, Arg-197, Asp-203, His-257, and Tyr-260) and the carboxylate group of the fatty acid along the trajectory were calculated using the *Hybrid* procedure developed by Gilson (1993). This method yields both accurate energies and fractional charges of titratable sites (Gilson, 1993).

(ester) or a product (fatty acid) molecule in the presence of a lipid aggregate. The presence of a lipid patch consisting of substrate molecules located around the lipid binding zone (Peters et al., 2000) causes that the active site lid opens wider than observed in an aqueous environment.

The structural and energetic analyses of the trajectories show some intriguing features revealing the origin of the interactions and the dynamic nature of substrate binding and product release. The behavior of the substrate or product molecule is sensitive to the solvent environment. Entering and leaving of substrate molecules were observed in the Rml-substrate-patch simulation, whereas in contrast, in a purely aqueous environment, the substrate molecule remained in the binding cleft (Peters et al., 2001a). Independent of the environment, the product molecule does not leave the pocket but shows different behavior. In an aqueous environment, the product remains in the binding cleft with the hydrophobic tail aligning to Leu-208–Pro-210. Contrarily, in the presence of the lipid aggregate, the tail of the fatty acid molecule points outward into the hydrophobic patch. The negative charge on the fatty acid is stabilized by interactions with the titratable residues Tyr-28, His-143, and His-257. Moreover, the carboxylate group forms hydrogen bonds with Ser-82, Ser-144, and Trp-88 persisting over the whole simulation period.

Monitoring the distances between the carboxylate group of the fatty acid and these residues indicate that tight hydrogen bounds are formed in particular with the serine residues. The tendency of the fatty acid to form hydrogen

bonds with Trp is less pronounced. The formation of hydrogen bonds between the fatty acid and residues in the binding pocket could be an important contribution to the mechanism by which product inhibition might take place. In a mixed monolayer of diglyceride (i.e., substrate) and fatty acid with as little as 0.1 mol % of fatty acid present, the hydrolysis rate slows down appreciably (Peters et al., 2000). The hydrogen-bonding sites in the binding pocket very likely function as anchoring points for the product when acting as an inhibitor. By analogy, the same type of analysis could be recommended for use by enzyme or ligand engineers who wish to design inhibitors for other serine hydrolases, which are of medical importance, e.g., hormone-sensitive lipase or serine proteases.

REFERENCES

Amadei, A., A. B. M. Linssen, and H. J. C. Berendsen. 1993. Essential dynamics of proteins. *Proteins Struct. Funct. Genet.* 17:412–425.

Antosiewicz, J., J. A. McCammon, and M. K. Gilson. 1994. Prediction of pH-dependent properties of proteins. *J. Mol. Biol.* 238:415–436.

Balsera, M. A., W. Wriggers, Y. Oono, and K. Schulten. 1996. Principal component analysis and long time protein dynamics. *J. Phys. Chem.* 100:2567–2572.

Berendsen, H. J. C., J. R. Grigera, and T. P. Straatsma. 1987. The missing term in effective pairs potentials. *J. Phys. Chem.* 91:6269–6271.

Bernstein, F. C., T. F. Koetzle, G. J. B. Williams, E. F. Meyer, M. D. Brice, J. R. Rogers, O. Kennard, T. Shimanouchi, and M. Tasumi. 1977. The protein data bank: a computer-based archival file for macromolecular structure. *J. Mol. Biol.* 112:535–542.

Brady, L., A. M. Brzozowski, Z. S. Derewenda, G. G. Dodson, S. Tolley, J. P. Turkenburg, L. Christiansen, B. Huge-Jensen, L. Norskov, L. Thim, and U. Menge. 1990. A serine protease triad forms the catalytic center of a triacylglycerol lipase. *Nature.* 343:767–770.

Brzozowski, A. M., U. Derewenda, Z. S. Derewenda, G. G. Dodson, D. M. Lawson, J. P. Turkenburg, F. Bjorkling, B. Huge-Jensen, S. A. Patkar, and L. Thim. 1991. A model for interfacial activation in lipases from the structure of a fungal lipase inhibitor complex. *Nature.* 351:491–494.

Burden, L. M., V. D. Rao, D. Murray, R. Ghirlando, S. D. Doughman, R. A. Anderson, and J. H. Hurley. 1999. The flattened face of type IIβ phosphatidylinositol phosphate kinase binds acidic phospholipid membranes. *Biochemistry.* 38:15141–15149.

Cantor, R. S. 1997. Lateral pressures in cell membranes: a mechanism for modulation of protein function. *J. Phys. Chem. B.* 101:1723–1725.

Davis, M. E., J. D. Madura, B. A. Luty, and J. A. McCammon. 1991. Electrostatics and diffusion of molecules in solution: simulations with the University of Houston Brownian dynamics program. *Comp. Phys. Commun.* 62:187–197.

Davis, M. E., and J. A. McCammon. 1991. *J. Comp. Chem.* 7:909–912.

Derewenda, U., A. M. Brzozowski, D. M. Lawson, and S. Z. Derewenda. 1992. Catalysis at the interface: the anatomy of a conformational change in a triglyceride lipase. *Biochemistry.* 31:1532–1541.

Derewenda, U., L. Swenson, R. Green, Y. Wei, G. G. Dodson, S. Yamaguchi, M. J. Haas, and Z. S. Derewenda. 1994a. An unusual buried polar cluster in a family of fungal lipases. *Nature Struct. Biol.* 1:36–47.

Derewenda, U., L. Swenson, Y. Wei, R. Green, P. M. Kobos, R. Joerger, M. J. Haas, and Z. S. Derewenda. 1994b. Conformational lability of lipases observed in the absence of an oilwater interface: crystallographic studies of enzymes from the fungi *Humicola lanuginosa* and *Rhizopus delemar*. *J. Lip. Res.* 35:524–534.

Derewenda, Z. S. 1994. *Lipases. Adv. Prot. Chem.* 45:1–52.

Desnulle, P., L. Sarda, and G. Ailhaud. 1960. Inhibition de la lipase pancreatique par le diethyl-*p*-nitrophenyl phosphate en emulsion. *Biochim. Biophys. Acta.* 37:570–571.

Dowhan, W. 1997. Molecular basis for membrane phospholipid diversity: why are there so many lipids? *Annu. Rev. Biochem.* 66:199–232.

Dumas, F., M. C. Lebrun, and J. F. Tocanne. 1999. Is the protein/lipid hydrophobic matching principle relevant to membrane organization and functions? *FEBS Lett.* 458:271–277.

Egloff, M. P., F. Marguet, G. Buono, R. Verger, C. Cambillau, and H. van Tilbeurgh. 1995. The 2.46 Å resolution structure of the pancreatic lipase-colipase complex inhibited by a C11 alkyl phosphonate. *Biochemistry.* 34:2751–2762.

Europort-D. 1997. Parallel version of GROMOS87 was developed by the Parallel Applications Centre, Southampton, England and installed on the 18 processor SGI Challenge at Novo Nordisk A/S.

Gilson, M. K. 1993. Multiple-site titration and molecular modeling: two rapid methods for computing energies and forces for ionizable groups in proteins. *Proteins Struct. Funct. Genet.* 15:266–282.

Honig, B., and A. Nicholls. 1995. Classical electrostatics in biology and chemistry. *Science.* 268:1144–1149.

Lindblom, G., and P. O. Quist. 1998. Protein and peptide interactions with lipids: structure, membrane function and new methods. *Curr. Opin. Coll. Interf. Sci.* 3:499–508.

Lindeberg, M., S. D. Zakharov, and W. A. Cramer. 2000. Unfolding pathway of the colicin el channel protein on a membrane surface. *J. Mol. Biol.* 295:679–692.

Madura, L. D., J. M. Briggs, R. C. Wade, M. E. Davis, B. A. Luty, A. Ilin, J. Antosiewicz, M. K. Gilson, B. Bagheri, L. R. Scott, and J. A. McCammon. 1995. Electrostatics and diffusion of molecules in solution: simulations with the University of Houston Brownian dynamics program. *Comp. Phys. Commun.* 91:57–67.

Mouritsen, O. G., and R. L. Biltonen. 1993. *In* Protein-Lipid Interactions. A. Watts, editor. Elsevier Science Publishing, New York. 1–39.

Mouritsen, O. G., and K. Jorgensen. 1998. A new look at lipid-membrane structure in relation to drug research. *Pharmacol. Res.* 15:1507–1519.

Muderhwa, J. M., and H. L. Brockman. 1992. Lateral lipid distribution as a major regulator of lipase activity. *J. Biol. Chem.* 267:24184–24192.

Panaiotov, I., M. Ivanova, and R. Verger. 1997. Interfacial and temporal organization of enzymatic lipolysis. *Curr. Opin. Coll. Interf. Sci.* 2:517–525.

Peters, G. H. 2001a. The dynamic response of a fungal lipase in the presence of charged surfactants. *Coll. Surf. B: Biointerfaces.* In press.

Peters, G. H., U. Dahmen-Levison, K. de Meijere, G. Brezesinski, S. Toxvaerd, H. Moehwald, A. Svendsen, and P. K. J. Kinnunen. 2000. Influence of surface properties of mixed monolayers on lipolytic hydrolysis. *Langmuir.* 16:2779–2788.

Peters, G. H., T. M. Frimurer, J. N. Andersen, and O. H. Olsen. 1999. Molecular dynamics simulations of protein-tyrosine phosphatase 1B: I. Ligand-induced changes in protein motions. *Biophys. J.* 77:505–515.

Peters, G. H., T. M. Frimurer, and O. H. Olsen. 1998. Electrostatic evaluation of the signature motif (H/V)CXSR(S/T) in protein-tyrosine phosphatases. *Biochemistry.* 37:5383–5393.

Peters, G. H., M. Ø. Jensen, and R. P. Bywater. 2001b. Dynamics of the substrate binding pocket in the presence of an inhibitor covalently attached to a fungal lipase. *J. Biomol. Struct. Dyn.* 19:1–14.

Peters, G. H., O. H. Olsen, A. Svendsen, and R. Wade. 1996a. Theoretical investigation of the dynamics of the active site lid in *Rhizomucor miehei* lipase. *Biophys. J.* 71:119–126.

Peters, G. H., S. Toxvaerd, N. B. Larsen, T. Bjørnholm, K. Schaumburg, and K. Kjaer. 1995a. Structure and dynamics of lipid monolayers: implicats for enzyme catalysed lipolysis. *Nature Struct. Biol.* 2:395–401.

Peters, G. H., S. Toxvaerd, O. H. Olsen, and A. Svendsen. 1995b. Modelling of complex biological systems: II. Effect of chainlength on the phase transitions observed in diglyceride monolayers. *Langmuir.* 11: 4072–4085.

Peters, G. H., S. Toxvaerd, O. H. Olsen, and A. Svendsen. 1997a. Computational studies of activation of lipases and the effect of a hydrophobic environment. *Protein Eng.* 10:137–145.

Peters, G. H., D. M. F. van Aalten, O. Edholm, S. Toxvaerd, and R. Bywater. 1996b. Dynamics of proteins in different solvent systems: analysis of essential motion in lipases. *Biophys. J.* 71:2245–2251.

Peters, G. H., D. M. F. van Aalten, A. Svendsen, and R. Bywater. 1997b. Essential dynamics of lipase binding sites: the effect of inhibitors of different chain length. *Protein Eng.* 10:149–155.

Prenner, E. J., R. N. A. H. Lewis, and R. N. McElhaney. 1999. The interaction of the antimicrobial peptide gramicidin S with lipid bilayer model and biological membranes. *Biochim. Biophys. Acta.* 1462: 201–221.

Sarda, L., and P. Desnuelle. 1958. Action de la lipase pancreatique sur les esters en emulsion. *Biochim. Biophys. Acta.* 30:513–521.

Seykora, J., M. M. Myatt, L. A. H. Allen, J. V. Ravetch, and A. Aderem. 1996. Molecular determinants of the myristol electrostatic switch of MARCKS. *J. Biol. Chem.* 271:18797–18802.

Subbiah, S. 1996. "Protein Motions." Molecular Biology Intelligence Unit. Springer Verlag, Heidelberg, Germany.

Thuren, T. 1988. A model for the molecular mechanism of interfacial activation of phospholipase A2 supporting the substrate theory. *FEBS Lett.* 229:95–99.

Tocanne, J. F., L. Dupou-Cezanne, and A. Lopez. 1994. Lateral diffusion of lipids in model and natural membranes. *Prog. Lipid Res.* 33:203–237.

van Aalten, D. M. F., A. Amadei, A. B. M. Linssen, V. G. H. Eijsink, and G. Vriend. 1995. The essential dynamics of thermolysin: confirmation of the hinge-bending motion and comparison of simulations in vacuum and water. *Proteins Struct. Funct. Genet.* 22:45–54.

van Aalten, D. M. F., J. B. C. Findlay, A. Amadei, and H. J. C. Berendsen. 1996. Essential dynamics of the cellular retinol-binding protein-evidence for ligand-induced conformational changes. *Protein Eng.* 8:1129–1135.

van Gunsteren, W. F., and H. J. C. Berendsen. 1987. GROMOS: Groningen molecular simulation computer program package. University of Groningen, The Netherlands.

van Tilbeurgh, H., M. P. Egloff, C. Martinez, N. Rugani, R. Verger, and C. Cambillau. 1993. Interfacial activation of the lipase-colipase complex by mixed micelles revealed by X-ray cryställography. *Nature.* 362:814–820.

Vriend, G. 1990. WHAT IF: a molecular modeling and drug design program. *J. Mol. Graph.* 8:52–56.

Warshel, A., and J. Åqvist. 1991. Electrostatic energy and macromolecular function. *Annu. Rev. Biophys. Chem.* 20:267–298.

Warshel, A., and S. T. Russell. 1984. Calculations of electrostatic interactions in biological systems and in solutions. *Quart. Rev. Biophys.* 17:283–422.

Weers, P. M. M., V. Narayanaswami, C. M. Kay, and R. O. Ryan. 1999. Interaction of an exchangeable apolipoprotein with phospholipid vesicles and lipoprotein particles. *J. Biol. Chem.* 274:21804–21810.

Winkler, F. K., A. D'Arcy, and W. Hunziker. 1990. Structure of human pancreatic lipase. *Nature.* 343:771–774.

Wulfson, E. X. 1994. *In* Lipases: Their Structure, Biochemistry, and Applications. P. Woolley and S.B. Petersen, editors. Cambridge University Press, Cambridge. 271–288.

Zidek, L., M. V. Novotny, and M. J. Stone. 1999. Increased protein backbone conformational entropy upon hydrophobic ligand binding. *Nature Struct. Biol.* 6:1118–1121.